AAPS PharmSciTech, Vol. 14, No. 2, June 2013 (© 2013)
DOI: 10.1208/s12249-013-9945-1

Research Article

Design of an Interpolyelectrolyte Gastroretentive Matrix for the Site-Specific Zero-Order Delivery of Levodopa in Parkinson's Disease

Ndidi C. Ngwuluka,[1] Yahya E. Choonara,[1] Girish Modi,[2] Lisa C. du Toit,[1] Pradeep Kumar,[1] Valence M. K. Ndesendo,[3] and Viness Pillay[1,4]

Received 5 December 2012; accepted 22 February 2013; published online 15 March 2013

Abstract. This study focused on developing a gastroretentive drug delivery system employing a triple-mechanism interpolyelectrolyte complex (IPEC) matrix comprising high density, swelling, and bioadhesiveness for the enhanced site-specific zero-order delivery of levodopa in Parkinson's disease. An IPEC was synthesized and directly compressed into a levodopa-loaded matrix employing pharmaceutical technology and evaluated with respect to its physicochemical and physicomechanical properties and *in vitro* drug release. The IPEC-based matrix displayed superior mechanical properties in terms of matrix hardness (34–39 N/mm) and matrix resilience (44–47%) when different normality's of solvent and blending ratios were employed. Fourier transform infrared spectroscopy confirmed the formation of the IPEC. The formulations exhibited pH and density dependence with desirable gastro-adhesion with Peak Force of Adhesion ranging between 0.15 and 0.21 N/mm, densities from 1.43 to 1.54 g/cm^3 and swellability values of 177–234%. The IPEC-based gastroretentive matrix was capable of providing site-specific levodopa release with zero-order kinetics corroborated by detailed mathematical and molecular modeling studies. Overall, results from this study have shown that the IPEC-based matrix has the potential to improve the absorption and subsequent bioavailability of narrow absorption window drugs, such as levodopa with constant and sustained drug delivery.

KEY WORDS: gastroretention; interpolyelectrolyte complex; levodopa; narrow absorption window drugs; Parkinson's disease.

INTRODUCTION

Despite the decades since the discovery of Parkinson's disease (PD), its treatment and management still poses a significant challenge. Anticholinergic drugs such as levodopa, selegiline, amantadine, bromocriptine, and catechol-*O*-methyltransferase inhibitors are used for the management of PD. Levodopa remains the gold standard and the most effective anti-parkinsonian agent eventually required by all patients with PD. Levodopa was for the first time injected into patients in 1961 (1). Subsequently, it was discovered that the absorption and bioavailability of levodopa was significantly reduced by metabolism through decarboxylation, *O*-methylation, transamination, and oxidation (2). Increasing the dose of levodopa and concomitant administration of levodopa with carbidopa, a decarboxylase inhibitor, were the early approaches employed to enhance the bioavailability of levodopa. However, larger doses increased the associated side-effects (3). Consequently, drug delivery technologies were employed to enhance the bioavailability of levodopa. Initially, immediate-release dosage forms were formulated in combination with decarboxylase inhibitors, such as carbidopa or benserazide. However, these immediate-release formulations produce erratic plasma levels of levodopa (4). In order to overcome these erratic plasma levels of levodopa, controlled release formulations were developed. Although the controlled release dosage forms improved on the erratic drug release profiles, they do not significantly enhance the bioavailability. Furthermore, the side-effects observed with controlled release dosage forms did not differ much from those of the immediate-release formulations (5).

Hence, further studies were undertaken to improve the bioavailability and subsequent therapeutic effect of levodopa. Pharmaceutical technologies have been one of the major approaches employed in this regard. Apart from immediate release and controlled release dosage forms; liquid formulations, dispersible tablets, oral disintegrating tablets, dual-release formulations, infusions, microspheres, implants, transdermal matrices, pulmonary, nasal, and rectal formulations have also been designed and developed to enhance the delivery of levodopa (6). However, many of these pharmaceutical approaches have not effectively enhanced the bioavailability of levodopa, reduced side-effects or produced constant plasma levels. While infusions may have enhanced the bioavailability and continuous

[1] Department of Pharmacy and Pharmacology, Faculty of Health Sciences, University of the Witwatersrand, 7 York Road, Parktown, 2193, Johannesburg, South Africa.
[2] Department of Neurology, Faculty of Health Sciences, University of the Witwatersrand, 7 York Road, Parktown, 2193, Johannesburg, South Africa.
[3] School of Pharmacy and Pharmaceutical Sciences, St. John's University of Tanzania, Dodoma, Tanzania.
[4] To whom correspondence should be addressed. (e-mail: Viness.Pillay@wits.ac.za)

dopaminergic stimulation, they still remain invasive and cumbersome for patients (6). Consequently, oral drug delivery is the most convenient route of administration and remains the major focus of research in optimally delivering levodopa. One of the challenges faced with levodopa is that the drug undergoes specific-site absorption mainly in the duodenum by a saturable facilitated transport mechanism specific to aromatic and branched amino acids (2). Hence, drug delivery technologies that can ensure continuous and prolonged delivery at this site by increasing the gastric residence time in order to improve the bioavailability are preferred. Controlled release gastroretentive drug delivery systems for narrow absorption window drugs can: (1) improve the absorption and bioavailability of these drugs over a prolonged period, (2) reduce the frequency of dosing, (3) target drugs required at the stomach or proximal small intestine hence reducing erratic concentrations of drug and side-effects, and (4) enhance the therapeutic efficacy (7). Hydrodynamically balanced systems are floating systems comprising levodopa and benserazide that have been developed and marketed for treating PD. However, the gastric residence time of such formulations was not significantly extended as anticipated, which may explain the similar pharmacokinetic profile it shares with the conventional controlled release formulations (8). Other gastrorententive drug delivery systems developed for the delivery of levodopa include unfolding multilayer delivery systems (8), multiple-unit sustained release floating minitablets (9) and coated multiple-unit sustained release floating minitablets (10). However, significant advancement in the treatment of PD with levodopa requires the development of an oral formulation that can improve the absorption and bioavailability of levodopa with constant therapeutic plasma concentrations.

Therefore, this study focused on developing a controlled release gastroretentive drug delivery system for the site-specific delivery of levodopa which may improve the absorption and bioavailability of levodopa as well as prevent erratic plasma levels by providing zero-order release for the management of PD. Furthermore, the study was undertaken to improve on the shortcomings of the various approaches of gastroretention by developing a triple-mechanism gastroretentive drug delivery system employing an interpolyelectrolyte complex (IPEC) to design a high density, swelling, and bioadhesive matrix for enhanced delivery of levodopa at a constant rate over a prolonged period of time. To characterize and evaluate the drug delivery system, a few pertinent characterization techniques such as Fourier transform infrared (FT-IR) spectroscopy, texture analyses, swellability testing, gastro-adhesivity testing, and *in vitro* drug release testing were employed.

MATERIALS AND METHODS

Materials

Eudragit® E100 (EUD; methacrylate copolymer; M_w= 47,000 g/mol, Evonik Röhm GmbH and Co. KG, Darmstadt, Germany), sodium carboxymethylcellulose (NaCMC M_w= 250 kDa, Fluka Biochemika, Buchs, Switzerland), locust bean (*Ceratonia siliqua*; M_w=310 kDa, Sigma-Aldrich, Steinheim, Germany), barium sulfate, potassium phosphate monobasic (KH_2PO_4), pullulan (PLLN; *Aureobasidium pullulans*; product number P4516), and 3-(3,4-dihydroxyphenyl)-L-alanine were purchased from Sigma-Aldrich Inc. (Steinheim, Germany). Acetic acid glacial, hydrochloric acid (HCl), sodium hydroxide (NaOH), silica, potassium chloride (KCl), and magnesium stearate were purchased from Merck Chemicals (Pty) Ltd. (Gauteng, South Africa). Ortho-phosphoric acid was obtained from BDH Chemicals (Poole, England).

Synthesis of the IPEC as a Gastroretentive Matrix Platform

EUD was milled and dissolved in 50-mL 0.1 N acetic acid while NaCMC was dissolved in 50-mL deionized water until homogenous mixtures were obtained. The EUD solution was then added into the NaCMC solution and agitated vigorously for 1–3 h. Thereafter, locust bean gum was added and agitated for 15 min. This formed an interpolymeric blend (IPB) that was subsequently lyophilized for 48 h and thereafter milled before direct compression to produce the gastroretentive matrix. The polymer ratios within the IPB are as shown in Table I. Formulations 1 and 3 that constituted EUD-NaCMC in the ratios of 1:0.5 and 0.5:1 respectively were further synthesized in 0.2, 0.4, 0.6, 0.8, and 1.0 N acetic acid.

Molecular Structural Component Determination of the IPEC

FT-IR spectra were obtained for the native polymers and the IPB using a PerkinElmer spectrometer (PerkinElmer Spectrum 100, Beaconsfield, UK) over a wavenumber range of 4,000–650 cm^{-1} to elucidate and confirm the structural modification of the IPB as a result of combining the native polymers EUD and NaCMC.

Direct Compression of the IPEC into a Gastroretentive Matrix

The IPB was directly compressed with the excipients listed in Table II using a Carver Hydraulic Press (Carver Industries Inc., Wabash, IN) at 3 tons. Blending of the components was undertaken in the following sequence: (1) relevant quantities of the IPB were added and blended in an alternating manner with the excipients, (2) silicon dioxide was firstly blended with some quantity of the IPB followed by the model drug levodopa, (3) PLLN and barium sulphate was then added, and (4) magnesium stearate was added and blended continuously for 2 min thereafter.

Table I. Compositions of the Polymers Utilized in the Ten Interpolyelectrolyte Complexes

Formulations (ratios)	Methacrylate copolymer (g)	Locust bean (g)	NaCMC (g)
F1 (1:1:0.5)	1.68	1.68	0.84
F2 (1:0.5:1)	1.68	0.84	1.68
F3 (0.5:1:1)	0.84	1.68	1.68
F4 (1:1:1)	1.4	1.4	1.4
F5 (2:1:0.5)	2.4	1.2	0.6
F6 (1:2:0.5)	1.2	2.4	0.6
F7 (0.5:1:2)	0.6	1.2	2.4
F8 (0.5:2:1)	0.6	2.4	1.2
F9 (2:0.5:1)	2.4	0.6	1.2
F10 (1:0.5:2)	1.2	0.6	2.4

Table II. Composition of the Directly Compressed IPEC-Based Gastroretentive Matrix

Components	Quantity (mg) per matrix
Levodopa	100
Polymeric blend (50%)	500
Pullulan (10%)	100
Magnesium stearate (1%)	10
Silica (silicon dioxide; 5.5%)	55
Barium sulfate	234

Determination of the Density of the Gastroretentive Matrix

The volume of the gastroretentive matrix was determined by obtaining its diameter and thickness using an electronic digital caliper (repeatability, 0.01 mm; Hangzhou United Bridge Tools Co Ltd., Zhejiang, China) while the mass was ascertained gravimetrically using a weighing balance (tarring range, 0–110 g; Denver Instrument Co., CO). Hence, the density for the matrix was computed after having obtained the mass and volume.

Evaluation of the Physicomechanical Strength of the Gastroretentive Matrix

The physicomechanical strength of the matrix was deduced from force-distance profiles using a Texture Analyzer (TA.XT*plus*, Stable Microsystems, Surrey, UK). The matrix hardness (MH) and deformation energy (DE) tests were performed using a 2-mm flat-tipped steel probe while matrix resilience (MR) analysis was performed with a 36 mm cylindrical probe fitted to the instrument. Data were captured through Texture Exponent Software (V3.2).

Gastro-adhesivity Testing of the Matrix

Freshly excised stomach tissue from a euthanized Large White pig model was obtained and equilibrated in 0.1 N HCl. The gastro-adhesive strength of the matrix was determined using a Texture Analyzer through Texture Exponent Software (V3.2) (TA.XT*plus*, Stable Microsystems, Surrey, UK). The Peak Force (PF) and the Work of Adhesion (WA) to separate the matrix from the tissue were used to assess the gastro-adhesivity of the matrix. The PF value is the maximum force required to detach the tissue from the matrix while the WA value was determined from the "area under the curve" between the force-distance profile (AUC_{FD}).

Assessment of the Matrix Swelling

The swelling of the matrix was determined in 0.1 N HCl. Briefly, the matrix was weighed, placed in pre-weighed wire baskets and immersed in 100 mL of 0.1 N HCl and placed in an orbital shaking incubator (LAS Equipment Co. (Pty) Ltd., South Africa) set at 37°C. The relative increase in mass was determined gravimetrically at time intervals over 24 h and the degree of swelling was subsequently determined using Eq. 1. Matrix swelling for each formulation was undertaken in duplicate with proximate results observed and the average reported.

$$\text{Degree of swelling} = \frac{M_t - M_0}{M_0} \quad (1)$$

Where, M_t is the mass of the matrix at time t, and M_0 is the initial mass of the matrix.

In Vitro Drug Release Studies

Drug release was assessed using USP dissolution apparatus II (Erweka DT700, Erweka GmbH, Heusenstamm, Germany). The temperature and stirring rate were maintained at 37±0.5°C and 50 rpm respectively while the dissolution media comprised 900 mL of 0.1 N HCl. The matrix was also tested in buffer media of pH 1.5 and 4.5. Samples (5 mL) were withdrawn at predetermined time intervals and replaced with the same volume of drug-free media to maintain sink conditions. The quantity of levodopa released was quantified using a UV spectrophotometer (Lambda 25 UV/Vis Spectrophotometer, PerkinElmer, MA). *In vitro* drug release studies were also performed by varying the normality of acetic acid in buffer pH 1.5 (standard buffer KCl/HCl), 4.5 (0.025 M KH_2PO_4/H_2PO_4), and 6.8 (standard buffer KH_2PO_4/NaOH) in order to visualize the behavior of the matrix within these media but not for determining the release of levodopa since it is unstable at these pH levels. Drug release studies were undertaken in duplicate within each medium for every formulation, and the average data are reported. Drug release profiles were further analyzed by kinetic modeling in terms of first-order, zero-order, Higuichi, Korsmeyer, and Peppas relationships.

Static Lattice Atomistic Simulations for Determination of Matrix Gastro-adhesivity

All molecular modeling computations were performed using HyperChem™ 8.0.8 Molecular Modeling (Hypercube Inc., Gainesville, FL) and ChemBio3D Ultra 11.0 (CambridgeSoft Corp., Cambridge, UK). The structure of PLLN (4 units saccharide) was built from standard bond lengths and angles using the Sugar Builder Module on HyperChem 8.0.8 while the structure of the mucopeptide analogue (MUC) was generated using the Sequence Editor Module. The models were energy minimized using a progressive convergence strategy where initially the MM+force field was used followed by energy-minimization using the Assisted Model Building and Energy Refinements (AMBER 3) force field. The conformer having the lowest energy was used to create the polymer–polymer and polymer–solvent complexes. A complex of one polymer molecule with another was assembled by disposing the molecules in parallel, and the same procedure of energy minimization was repeated to generate the final models: PLLN, MUC, and PLLN-MUC. Full geometrical optimization was performed in vacuum employing the Polak–Ribiere conjugate gradient algorithm until an RMS gradient of 0.001 kcal/mol was reached. For molecular mechanics computations in vacuum, the force fields were utilized with a distance-dependent dielectric constant scaled by a factor of 1. The 1–4 scale factors used were electrostatic 0.5 and van der Waals 0.5 (11).

RESULTS AND DISCUSSION

Synthesis of the IPEC

Upon blending transparent EUD and NaCMC solutions, white strand-like precipitates were produced within the gel matrix for the combination ratios of 1:0.5 and 1:1 of EUD and NaCMC, respectively. This indicated incomplete interaction at such ratios. Hence at the end of 3 h, the product resembled an entangled gel with whitish strands. However, at the stoichiometrical ratio of 0.5:1 of EUD and NaCMC, respectively, an insoluble homogenous white blend was produced. At a 0.5:1 ratio, cationic EUD and anionic NaCMC interacted to form an IPEC. The IPEC formed was a distinct blend with no significant physical transition of the blend observed with the addition of locust bean apart from an increase in viscosity. However, based on computational modeling, although locust bean is a neutral galactomannan polymer (12,13), it acted as a linker between EUD and NaCMC with intermolecular H bonding. The hydrophilic groups of locust bean displayed affinity to existing H_2O molecules that led to a further increase in viscosity as locust bean gum swelled. The H_2O molecules within the IPEC sublimated during the lyophilization process resulting in an anhydrous porous scaffold-like IPEC. Observably, the degree of porosity increased with an increase in the normality of acetic acid; although, after lyophilization, the scaffold-like IPEC was milled for direct compression.

Spectroscopic Chemical Structure Analysis of the IPEC

FT-IR spectra obtained for the native polymers (EUD and NaCMC) are shown in Fig. 1a while the chemical structural transitions for various compositions of the IPEC are shown in Fig. 1b–e. The characteristic peaks for EUD were found at 2,821.42, 1,725, 1,270.38, 1,239.56, 1,143.69, 962.05, 842.49, and 747.81 cm^{-1}, and those of NaCMC were identified at 3,210.04, 1,587.18, 1,411.77, 1,321.86, and 1,019.59 cm^{-1}. The blend between EUD and NaCMC produced a chemical interaction as evidenced by the spectra obtained, while incorporation of locust bean resulted in a physical interaction. The chemical interactions between EUD and NaCMC led to the disappearance or diminished characteristic peaks of EUD at the homogenous blend ratio of 0.5:1 as found in formulation F3. This modification in the structure of EUD altered its solubility in acid and thereby responsible for the modification of the rate of levodopa release in acidic medium. The aliphatic aldehyde peaks of EUD at 2,821.42 and 2,769.84 cm^{-1} disappeared in formulation F3 but was still visible in formulations F1 (1:0.5) and F2 (1:1). The other formulations were based on the same ratios 1:0.5 and 1:1, 0.5:1 of EUD/NaCMC, respectively. Hence, the focus was directed to the formulations, F1, F2, and F3. The peak for EUD at 747 cm^{-1} that was present in both F1 and F2 disappeared in F3. However, the distinct carbonyl peak at 1,725 cm^{-1} diminished in F3 while it was still very pronounced in F2 and F3. This indicated that a few carbonyl groups were involved in the interaction while the aliphatic aldehyde groups were converted to aliphatic alcohols that sublimated during the lyophilization process. The peak at 1,143.69 cm^{-1} for EUD shifted to 1,145.59 cm^{-1} but remained distinct in F1 and F2 while in F3 it appeared as a shoulder to the characteristic peak of NaCMC at 1,019.12 cm^{-1}, which also shifted from 1,019.59 cm^{-1}. The impact of locust bean on the chemical structural modification could not be seen from the spectra except for that of F1 which had a peak at 868.06 cm^{-1} which was typical to locust bean as shown in Fig. 1a. This may be due to the fact that F1 was more of a heterogeneous blend. Furthermore, it was envisaged that the homogeneity of F3 resulted in an almost superimposed spectra (Fig. 1e) with very slight differences in the degree of absorbance at the various frequencies or peaks with F3 in 1.0 N acetic acid having the highest degree of absorbance at peaks 1,725, 1,589, 1,408, 1,268.50, and 1,019 cm^{-1}. This was indicative of the impact of varying the normality of acetic acid which may influence the behavior of the IPEC in terms of the degree of swelling, matrix erosion and subsequent drug release. In contrast, spectra obtained for F1 were not superimposed since the differences in the degree of absorbance for each spectrum were distinct. Polymer modification in this case polymer−polymer interaction altered the properties of the native polymers to enhance the drug delivery properties. The IPEC obtained was therefore suited to improve the release of levodopa over a prolonged period at a fairly constant rate due to a possible change in matrix behavior and performance of the IPEC in dissolution media.

Direct Compression of the IPEC into a Gastroretentive Matrix

IPEC compositions were directly compressible and not friable. This indicated that additional compaction enhancing excipients were not required for formulation the gastroretentive matrix. Excipients that were added included a density enhancing agent ($BaSO_4$), silica as a glidant and magnesium stearate as a lubricant to improve the flow properties of the IPEC during gastroretentive matrix manufacture by direct compression. PLLN was added as a bioadhesive agent. The IPEC showed desirable compactibility and compressibility at 2 and 3 tonnes of compression with no evidence of capping or lamination.

Density Analysis of the IPEC-Based Gastroretentive Matrix

The matrix density determination of each formulation is shown in Table III. The density values ranged between 1.43 and 1.54 g/cm^3. This was indicative of the ability of the matrix to sink down to the antrum of the stomach due to being significantly denser than the typical gastric content within the stomach. Although a density value of >2.4 g/cm^3 is advocated for high-density delivery systems to ensure prolonged gastric residence time (14,15), it was envisaged that the IPEC-based matrices will still provide gastric residence with a density value less than recommended since the matrix constitutes three mechanisms of gastroretention (1) high density, (2) swellability, and (3) gastro-adhesivity. From physiological studies, it can be deduced that nondisintegrating single-unit drug delivery systems would remain in the stomach in the fed phase and would be emptied via peristalsis (16). Drug delivery systems are more prone to clear from the stomach at fasted-state than fed state due to peristalsis. Hence, the IPEC-based matrix with a density value of 1.4 g/cm^3 and nondisintegrating at stomach pH, when ingested, will sink to the antrum of the stomach and will be emptied only during peristalsis. However, it was envisaged that the ability of the IPEC-based matrix to swell beyond the size of the pylorus and its gastro-adhesivity would facilitate retention of the matrix in the stomach even beyond the period of peristalsis.

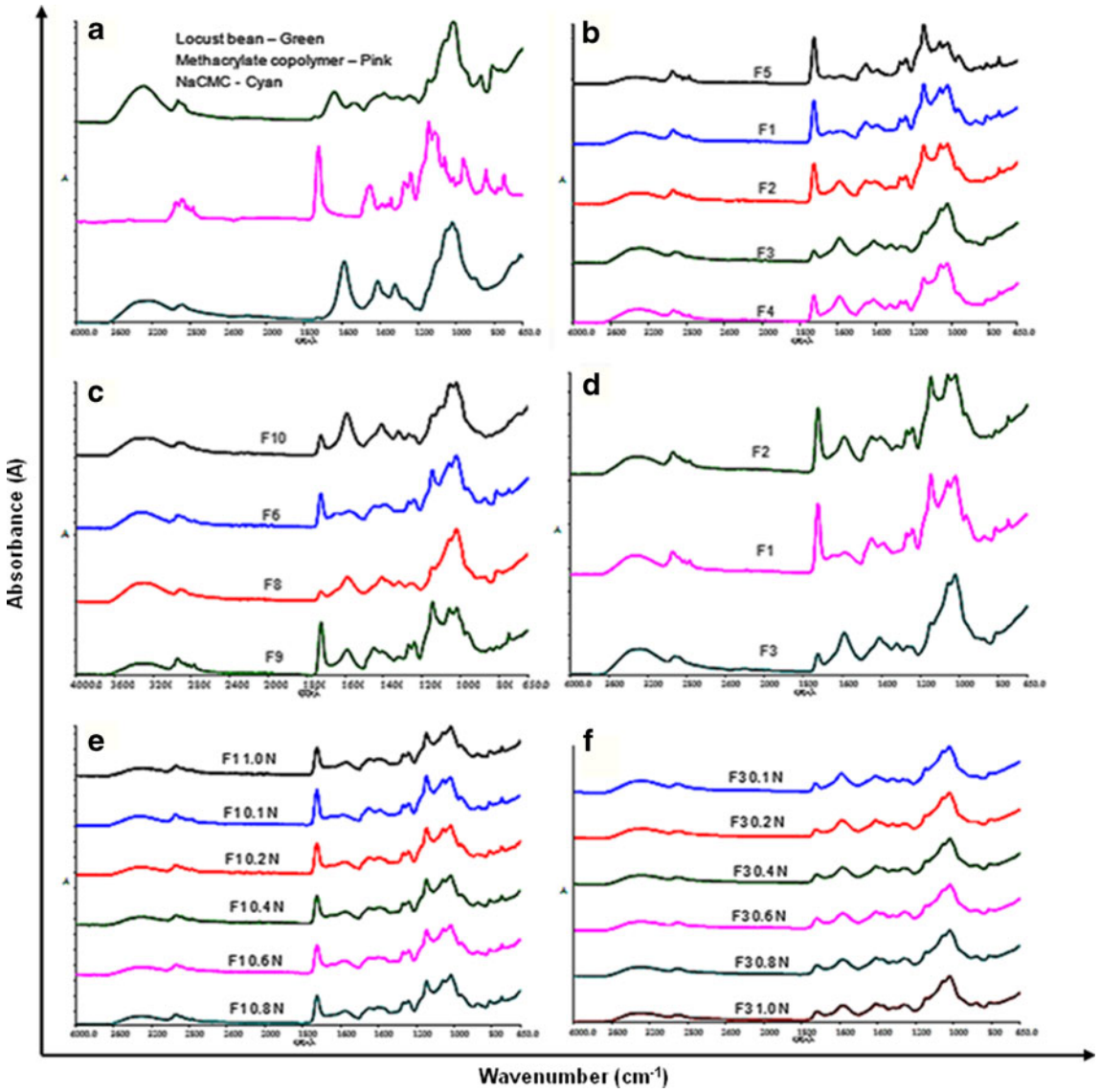

Fig. 1. FT-IR spectra for the IPEC: **a** native polymers namely locust bean, EUD, and NaCMC; **b** formulations F1–5; **c** formulations F6–10; **d** formulations F1–3; **e** formulation F1 in varying normality of acetic acid; and **f** formulation F3 in varying normality of acetic acid

Physicomechanical Property Analyses of the IPEC-Based Gastroretentive Matrix

Physicomechanical property analyses was undertaken since the MH, DE, and MR are indicative of the stability of the IPEC-based matrix and the ability to withstand pressure during direct compression and to restore its original dimensions after compressional stress applied during textural analysis. MH and MR also indicate the degree of matrix density and porosity which affects the drug release profile by transitioning the rate of dissolution medium influx into the matrix (17). A lower MH and MR may indicate the presence of voids which collapse on application of stress. Porosity also determines the quantity of DE required to alter the matrix. The harder the matrix, the less the energy absorbed or the more the DE which also affects the MR. The inherent properties of the polymers utilized in the formulation of the matrix also determines the degree of hardness. Furthermore, in the course of this study, it was also observed that lyophilization may have contributed to matrix strengthening. Native polymers which would not ordinarily retain a 3D network after matrix formation would do so through lyophilization. The different formulations as shown in Table IV indicated superior MH values that ranged from 34.720 to 39.707 N/mm; DE values from 0.012 to 0.014 Nm while MR ranged from 44.25 to 47.65%. Overall, all formulations had desired physicomechanical strength **(**MH=30–40 N/mm; DE=0.012–0.015 Nm; and MR=45–50%**)** and therefore would be able to withstand the pressures of manufacture and use. Typical force-distance and force-time profiles obtained are shown in Fig. 2.

Gastro-adhesivity Testing of the IPEC-Based Gastroretentive Matrix

The IPEC-based matrices from different polymer ratios and normality of acetic acid were found to be gastro-adhesive as shown in Figs. 3a–b and 4a–c. The interactions between the

Table III. Densities of the IPEC-Based Gastroretentive Matrices

Formulation	Density (mg/mm^3 or g/cm^3)
F1	1.51
F2	1.54
F3	1.50
F4	1.54
F5	1.50
F6	1.50
F7	1.51
F8	1.50
F9	1.52
F10	1.51
F1 0.2N	1.52
F1 0.4N	1.47
F1 0.6N	1.46
F1 0.8N	1.52
F1 1.0N	1.50
F3 0.2N	1.45
F3 0.4N	1.43
F3 0.6N	1.47
F3 0.8N	1.48
F3 1.0N	1.50

F1 0.2N formulation F1 synthesized in 0.2 N acetic acid, *F3 0.4N* formulation F3 synthesized in 0.4 N acetic acid, etc.

gastric mucosal surfaces and drug delivery systems formulated from bioadhesive polymers include covalent bonding, H bonding, electrostatic forces, such as Van der Waal forces, chain interlocking, and hydrophobic interactions (18,19). These interactions are regulated by pH and ionic conditions. The degree of interaction between the polymers and mucus is also dependent on the mucus viscosity, degree of entanglement and water content (18). Upon increasing the applied force from 0.5 to 1 N, the peak adhesive force (PAF) and work of adhesion (WA) increased. Increased applied force normally increases intimate contact by causing viscoelastic deformation at the interface between the mucus and the drug delivery system (18). Although the contact time employed was 5 s, the gastro-adhesive results were commensurable and if contact time was increased, there would have been a subsequent increase in the interaction of the polymeric chains with the mucus which would have led to an increased gastro-adhesion. The PAF and WA values were found to be higher when the IPEC-based matrices adhered to the gastro-epithelium. This may have been enhanced by the presence of the microbial bioadhesive agent, PLLN from *A. pullulans* included within the matrices. Microbial adhesions are postulated to have the capability of increasing mucoadhesion to the epithelium (20). It is envisaged that the incorporation of PLLN within the IPEC-based gastroretentive matrix would overcome the challenge of rapid mucus turnover thereby prolonging gastric residence time since it can adhere to the gastro-epithelial cells.

Table IV. Texture Analysis Results for the IPEC-Based Gastroretentive Matrices

Formulation	Matrix hardness (N/mm)	Deformation energy (Nm)	Matrix resilience (%)
F1	39.364	0.012	45.39
F2	38.419	0.012	44.25
F3	38.919	0.012	46.68
F4	38.897	0.012	46.23
F5	39.707	0.012	46.52
F6	38.367	0.012	46.86
F7	37.042	0.012	46.79
F8	37.07	0.012	47.65
F9	38.403	0.012	45.43
F10	35.769	0.013	47.65
F1 0.2N	37.317	0.012	46.75
F1 0.4N	37.961	0.013	47.22
F1 0.6N	36.497	0.013	46.15
F1 0.8N	36.316	0.013	46.80
F1 1.0N	36.683	0.013	46.37
F3 0.2N	35.349	0.013	46.25
F3 0.4N	34.72	0.013	46.36
F3 0.6N	34.937	0.013	46.72
F3 0.8N	35.027	0.014	45.98
F3 1.0N	36.393	0.013	46.32

F1 0.2N formulation F1 synthesized in 0.2 N acetic acid, *F3 0.4N* formulation F3 synthesized in 0.4 N acetic acid, etc.

Assessment of the IPEC-Based Matrix Swelling

Drug release kinetics from a polymeric matrix is affected by structural features of the polymer network, the process of hydration, swelling and degradation of the polymer(s) (21). As the dissolution medium is absorbed by the matrix, it swells; the incorporated drug dissolves and diffuses through the pores and out of the matrix. The rate of diffusion depends on the degree of swelling thereby affecting the quantity of drug released with time. The swelling process is affected by the polymer-solvent interaction, presence of drug and degree of crosslinking (22). Increasing the degree of crosslinking would lower the degree of swelling thereby reducing water content and subsequent diffusion of drug from the hydrogel (23). Matrices formulated with purely EUD dissolved in acidic medium while pure NaCMC matrices swelled to 384% its original size with loss of its 3D network. However, the IPEC (EUD-NaCMC) swelled to an even greater extent than NaCMC (465%) and maintained its 3D network. On addition of locust bean gum, the hydrophilic groups developed affinity for the available H_2O holding capacity of the IPEC thereby reducing the degree of swelling of the blend to <300%. Table V list the degree of swelling obtained for the various formulations at $t_{24\ h}$. However, formulation F3 was selected to determine the degree of swelling at time intervals over 24 h. Formulation F3 was selected since an ideal IPEC was obtained at that ratio (0.5 EUD/1.0 NaCMC) and Fig. 5a depicts the degree of swelling profile over 24 h. It was observed that the degree of swelling decreased as the normality of acetic acid increased from 229% (0.1 N acetic acid) to 202% (1.0 N acetic acid) (Fig. 5b). Consequently, it was expected that the rate of levodopa release from the IPEC-based gastroretentive matrix will decrease as the normality of acetic acid increases.

In Vitro Drug Release Analysis

Desirable release profiles of levodopa were obtained as depicted in Fig. 6a–e. Notably, the 3D network of the matrix was retained over the 24-h period of the study. However, on physical touch of the hydrated matrices following dissolution, it was observed that F5 was the softest purportedly due to

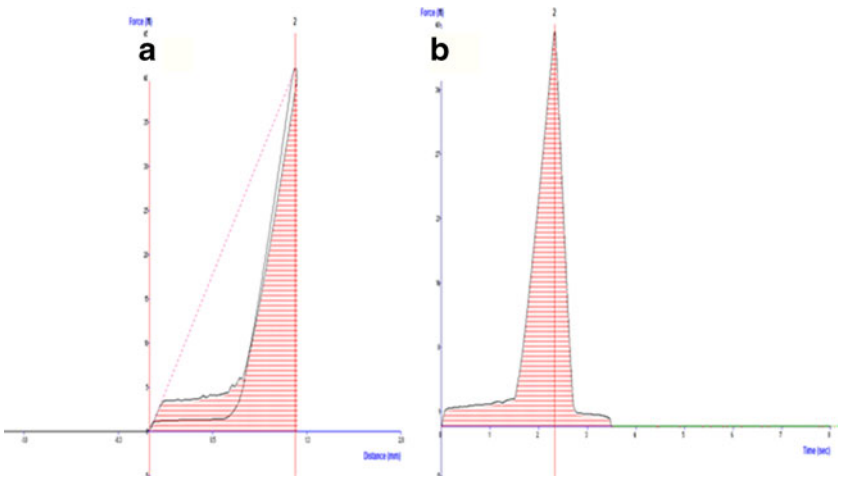

Fig. 2. Typical force-distance and force-time profiles of the IPEC for determining **a** matrix hardness (gradient) and DE (AUC) and **b** MR

higher concentration of EUD which was three times greater than the concentration of NaCMC with weak associations since more NaCMC is required for stronger interactions. The matrices that required pressure on touch in order to collapse were F3, F7, and F10 which was most certainly due to the presence of more NaCMC in the formulation than EUD. In

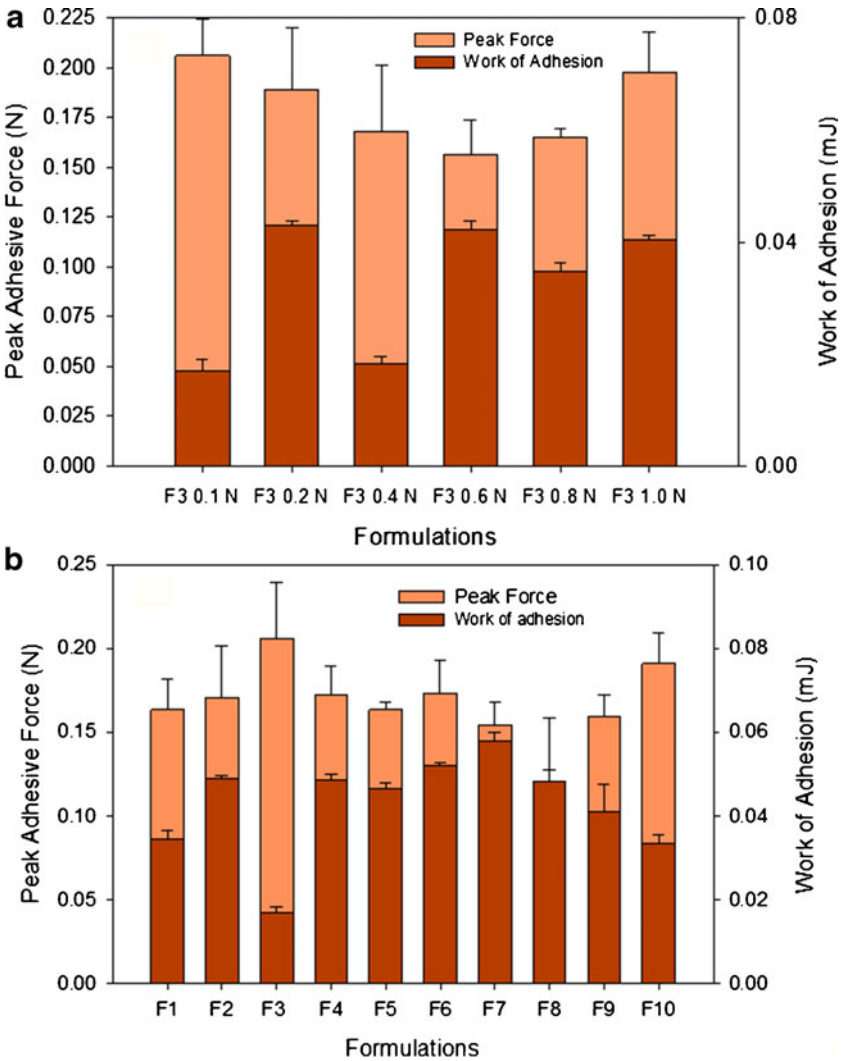

Fig. 3. Gastro-adhesive profiling of **a** formulation F3 and **b** formulations F1–10 in different normality of acetic acid (applied force=1 N; *N*=3)

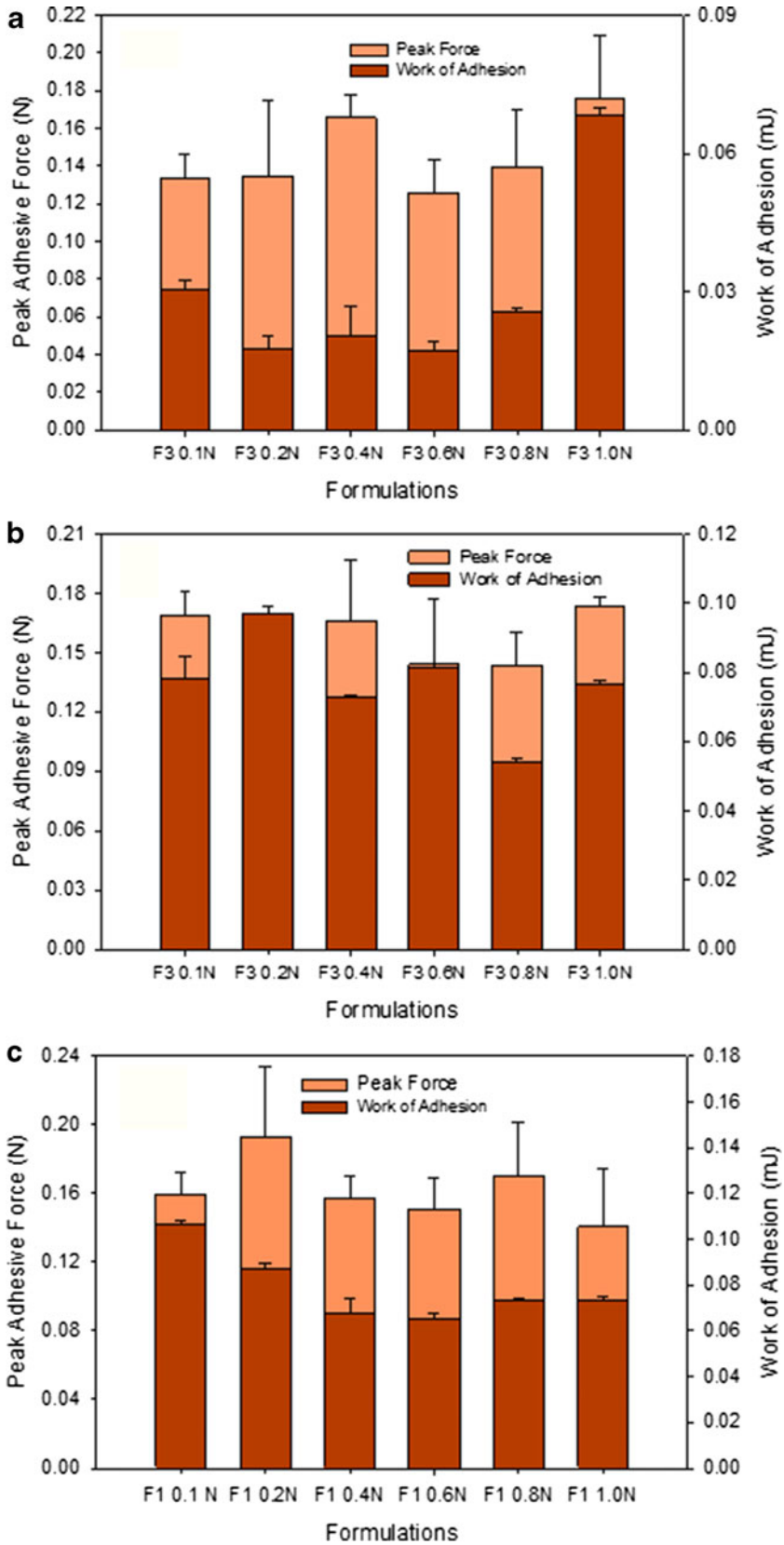

Fig. 4. **a** Gastro-adhesive profiling, **b** epithelial adhesive profiling of formulation F3, and **c** epithelial adhesive profiling of formulation F1 in different normalities of acetic acid (applied force=0.5N; *N*=3)

Table V. Degree of Swelling of IPEC-Based Gastroretentive Matrices

Formulation	Degree of swelling (%)
F1	221.30
F2	187.91
F3	218.19
F4	204.62
F5	220.10
F6	241.36
F7	200.81
F8	211.63
F9	177.36
F10	183.36
F1 0.2N	216.46
F1 0.4N	218.50
F1 0.6N	203.90
F1 0.8N	218.85
F1 1.0N	234.25

F1 0.2N formulation F1 synthesized in 0.2 N acetic acid, *F3 0.4N* formulation F3 synthesized in 0.4 N acetic acid, etc.

Fig. 6a, b, the levodopa release profiles of formulations F3, F7, and F10 are distinct from other formulations that were more aligned. The degree of crosslinking in the matrices for which the profiles slightly aligned may have been due to weak interactions and minimal salt generation during synthesis of the IPEC. The mechanism of drug release was clearly by swelling, dissolution, and diffusion of levodopa since the matrices retained their 3D network in 0.1 N HCl and buffer of pH 1.5. This was confirmed by mathematical modeling shown in Table VI. F1 was selected and synthesized in different normality's of acetic acid. However, not much difference was observed as the profiles were practically aligned as depicted in Fig. 6c. Although there were increased acetate ions as the normality increased, the required salt for threshold crosslinking was not generated due to the lower concentration of NaCMC. However, differences in levodopa release could be seen when F3 was selected for altering the normality in acetic acid (Fig. 6d). The differences depicted by the profiles indicated the varying degree of crosslinking with varying normality's of acetic acid. The matrices in dissolution media 0.1 N HCl and buffer pH 1.5 (standard buffer KCl/HCl) generated desirable levodopa release profiles as depicted in Fig. 6d, e and still retained their 3D network. Hence, the mechanisms of drug release involved in these media were matrix swelling and dissolution followed by the subsequent diffusion of levodopa from the matrix.

Interestingly, as the pH increased to 4.5, the matrices underwent gradual swelling with surface erosion throughout the 24-h period indicating that the drug release mechanism from the IPEC-based matrices was pH dependent. Consequently, the drug release profiles at pH 4.5 as shown in Fig. 6f differed from those obtained at pH 1.5 or 0.1 N HCl (Fig. 6d, e). Surface erosion occurred when the rate of erosion was greater than the rate of hydration (rate of absorption of dissolution medium) and occurred at constant velocity which lead to reproducible kinetics of erosion and levodopa release that essentially followed zero-order kinetics (24,25). Hence, the mechanism of drug release at pH 4.5 was principally surface erosion, matrix swelling, dissolution and subsequently diffusion of levodopa from the matrix thus producing zero-order release profiles. Figure 7 shows digital images of F3 at pH 1.5 and 4.5. It was observed that the matrices did not completely erode at the 24th hour. However, the degree of erosion decreased as the normality of acetic acid increased which in turn affected the drug release profile as well as the fractional drug released at the 24th hour as shown in Fig. 6f. A more linear drug release profile (zero order) was obtained for F3 in 0.1 N acetic acid which eroded more than the other formulations, indicating that erosion may have been its principal mechanism of drug release. In addition, dissolution was undertaken at pH 6.8, the focus was not on the drug release but rather on the behavior of the IPEC-based matrices. This was undertaken since the model drug, levodopa, is known to be unstable at pH 6.8 and therefore the fractional drug release was not obtained. However, it was observed that the matrices underwent surface erosion as well over 24 h. Hence the technology employed in synthesizing the IPEC may be explored for further development of drug delivery devices for application where constant rate of delivery is required in other sites of the gastrointestinal tract.

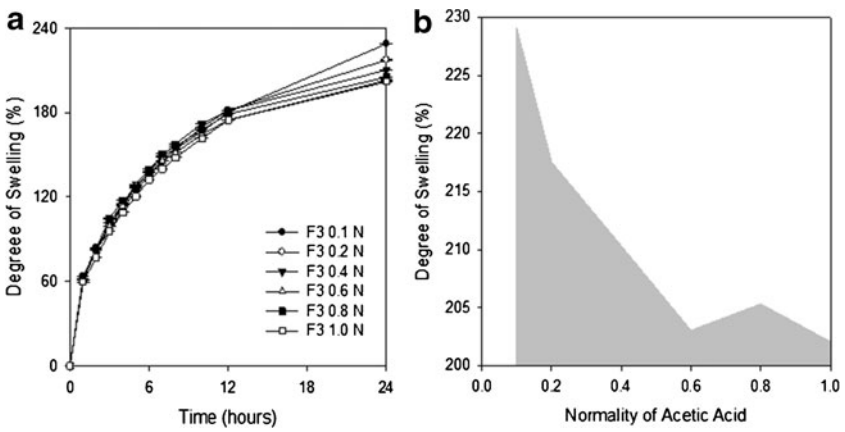

Fig. 5. **a** Degree of swelling (in percent) for formulation F3 in varying normalities of acetic acid and **b** relationship between normality of acetic acid and the degree of swelling (in percent)

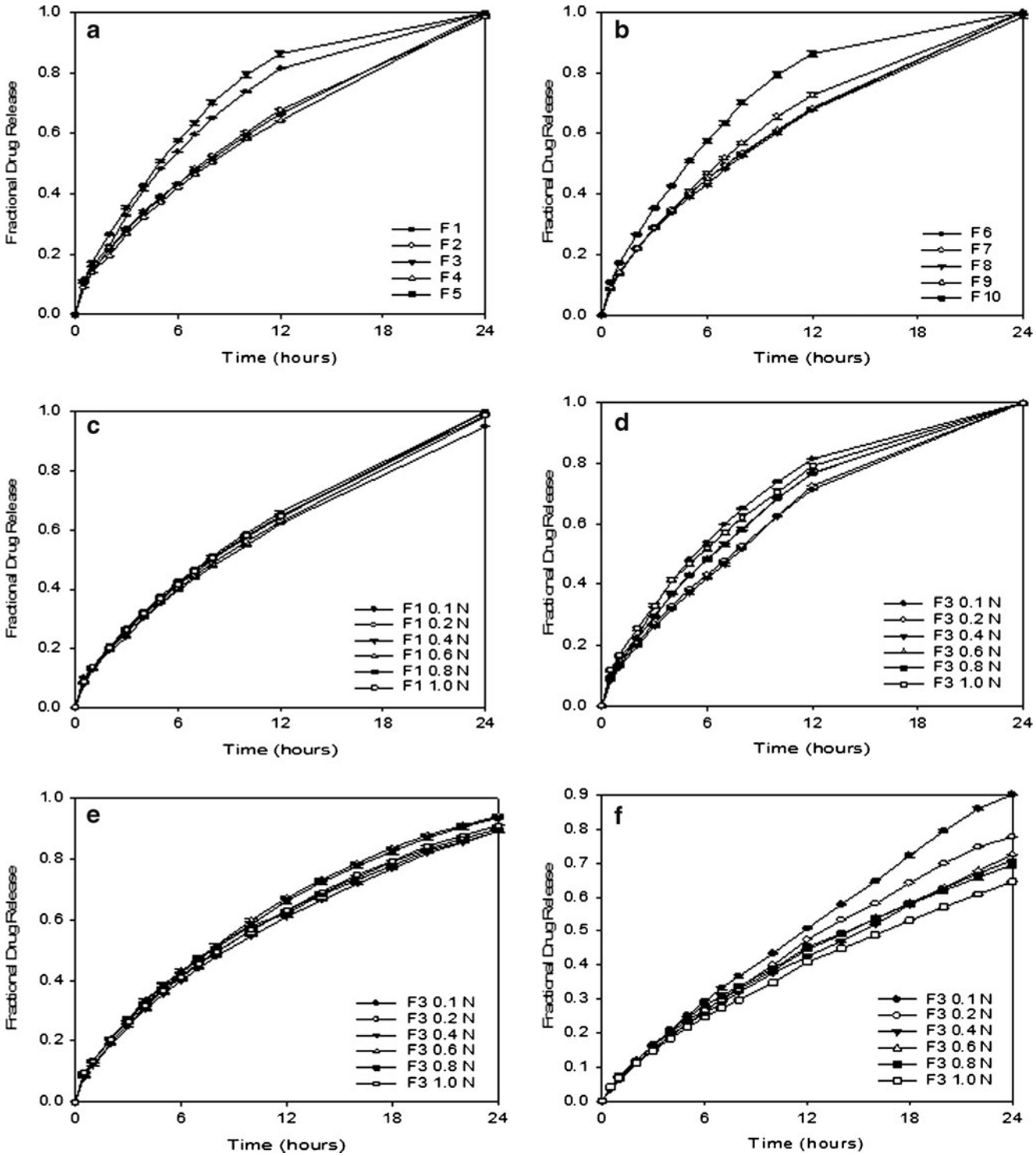

Fig. 6. Drug release profiles of **a** formulations F1–5 (0.1 N HCl), **b** F6–10 (0.1 N HCl), **c** F1 in different normalities of acetic acid (0.1 N HCl), **d** F3 in different normalities of acetic acid (0.1 N HCl), **e** F3 in different normalities of acetic acid (buffer pH 1.5), and **f** F3 in different normalities of acetic acid (buffer pH 4.5)

Mathematical Modeling of Drug Release Profiles

The drug release profiles were fitted into zero- and first-order kinetic algorithms, and the data are shown in Table VI. The zero- and first-order models used are shown in Eqs. 2 and 3.

$$f_t = K_0 t \tag{2}$$

Where f_t is the fraction of drug released in time t and K_0 is zero-order constant. The zero-order release constant and the regression squared were obtained by plotting fractional drug released *versus* time.

$$In\ Q_t = In\ Q_0 K_1 t \tag{3}$$

Table VI. Mathematical Modeling of Levodopa Release from the IPEC-Based Gastroretentive Matrices

	Zero order			First order			Higuichi			Korsmeyer–Peppas				
Drug device	k_0	r	r^2	K_1	r	r^2	K_H	r	r^2	K_{KP} (h^{-n})	r	r^2	n	Best-fit model
F1	4.8486	0.9854	0.9711	−0.0321	0.9993	0.9987	18.0585	0.9928	0.9856	13.7468	0.9953	0.9907	0.58	First order
F2	5.0202	0.9858	0.9719	−0.0339	0.9993	0.9987	18.6906	0.9928	0.9857	13.4927	0.9969	0.9938	0.61	First order
F3	6.6207	0.9820	0.9644	−0.0581	0.9974	0.9948	24.7393	0.9926	0.9853	16.5501	0.9941	0.9883	0.65	First order
F4	5.0831	0.9827	0.9658	−0.0347	0.9999	0.9998	19.0121	0.9943	0.9874	14.3913	0.9960	0.9920	0.59	First order
F5	5.1749	0.9817	0.9637	−0.0362	0.9994	0.9989	19.4002	0.9955	0.9910	15.4241	0.9974	0.9948	0.57	First order
F6	5.3714	0.9801	0.9605	−0.0382	0.9996	0.9992	20.1668	0.9953	0.9907	15.0418	0.9946	0.9893	0.60	First order
F7	5.8944	0.9853	0.9708	−0.0448	0.9992	0.9983	21.9533	0.9926	0.9853	13.5738	1.0000	1.0000	0.69	Korsmeyer–Peppas
F8	5.3556	0.9820	0.9643	−0.0379	0.9991	0.9983	20.0664	0.9952	0.9905	13.8867	0.9999	0.9997	0.64	Korsmeyer–Peppas
F9	5.4391	0.9807	0.9618	−0.0389	0.9996	0.9992	20.4124	0.9956	0.9912	14.1612	1.0000	0.9999	0.64	Korsmeyer–Peppas
F10	7.0665	0.9815	0.9634	−0.0691	0.9946	0.9892	26.4468	0.9937	0.9874	17.0805	0.9997	0.9994	0.67	Korsmeyer–Peppas
F1 0.1N	4.8486	0.9854	0.9711	−0.0321	0.9993	0.9987	18.0585	0.9928	0.9856	13.7468	0.9953	0.9907	0.58	First order
F1 0.2N	5.0119	0.9845	0.9693	−0.0321	0.9993	0.9987	18.7028	0.9938	0.9876	12.3538	1.0000	0.9999	0.66	Korsmeyer–Peppas
F1 0.4N	5.1390	0.9849	0.9700	−0.0350	0.9997	0.9995	19.1665	0.9936	0.9872	12.7175	1.0000	0.9999	0.65	Korsmeyer–Peppas
F1 0.6N	5.1336	0.9848	0.9698	−0.0351	0.9996	0.9992	19.1522	0.9938	0.9877	13.0617	0.9999	0.9998	0.64	Korsmeyer–Peppas
F1 0.8N	5.2315	0.9840	0.9682	−0.0363	0.9995	0.9990	19.5433	0.9943	0.9887	13.4462	0.9999	0.9997	0.64	Korsmeyer–Peppas
F1 1.0N	5.1394	0.9836	0.9676	−0.0352	0.9997	0.9995	19.2091	0.9945	0.9890	13.5052	0.9998	0.9996	0.63	Korsmeyer–Peppas
F3 0.1N (HCl)	6.6207	0.9820	0.9644	−0.0581	0.9974	0.9948	24.7393	0.9926	0.9853	16.5501	0.9941	0.9883	0.65	First order
F3 0.2N (HCl)	5.6743	0.9905	0.9810	−0.0426	0.9925	0.9850	20.9499	0.9892	0.9785	13.6584	0.9998	0.9995	0.64	Korsmeyer–Peppas
F3 0.4N (HCl)	5.6414	0.9920	0.9840	−0.0418	0.9931	0.9863	20.7605	0.9874	0.9750	12.9003	0.9998	0.9995	0.66	Korsmeyer–Peppas
F3 0.6N (HCl)	6.1587	0.9870	0.9741	−0.0495	0.9960	0.9920	22.8820	0.9919	0.9839	14.5211	0.9995	0.9990	0.67	Korsmeyer–Peppas
F3 0.8N (HCl)	6.1349	0.9873	0.9748	−0.0493	0.9957	0.9914	22.7806	0.9917	0.9835	14.7537	0.9987	0.9973	0.66	Korsmeyer–Peppas
F3 1.0N (HCl)	6.2179	0.9795	0.9594	−0.0521	0.9968	0.9936	23.3766	0.9961	0.9922	17.4703	0.9987	0.9974	0.61	Korsmeyer–Peppas
F3 0.1N (1.5)	3.5204	0.9704	0.9416	−0.0374	0.9968	0.9937	19.5399	0.9973	0.9946	12.3396	0.9982	0.9963	0.67	Korsmeyer–Peppas
F3 0.2N (1.5)	3.5275	0.9745	0.9497	−0.0386	0.9955	0.9911	19.5139	0.9982	0.9965	13.5457	0.9997	0.9994	0.62	Korsmeyer–Peppas
F3 0.4N (1.5)	3.5094	0.9780	0.9565	−0.0371	0.9940	0.9881	19.3333	0.9976	0.9953	12.3823	0.9997	0.9994	0.65	Korsmeyer–Peppas
F3 0.6N (1.5)	3.7475	0.9747	0.9500	−0.0474	0.9903	0.9807	20.7090	0.9973	0.9947	14.0056	0.9989	0.9978	0.62	Korsmeyer–Peppas
F3 0.8N (1.5)	3.7072	0.9752	0.9509	−0.0458	0.9903	0.9807	20.4827	0.9977	0.9953	14.0475	0.9989	0.9977	0.62	Korsmeyer–Peppas
F3 1.0N (1.5)	3.5844	0.9773	0.9550	−0.0403	0.9934	0.9868	19.7611	0.9976	0.9953	13.7784	0.9989	0.9979	0.61	Korsmeyer–Peppas
F3 0.1N (4.5)	3.7339	0.9974	0.9948	−0.0381	0.9722	0.9452	19.8343	0.9810	0.9624	6.5073	0.9996	0.9993	0.83	Korsmeyer–Peppas
F3 0.2N (4.5)	3.2566	0.9948	0.9896	−0.0266	0.9950	0.9900	17.4162	0.9851	0.9704	6.0007	0.9998	0.9997	0.83	Korsmeyer–Peppas
F3 0.4N (4.5)	2.8601	0.9928	0.9857	−0.0211	0.9971	0.9943	15.3880	0.9891	0.9783	6.4209	0.9993	0.9986	0.77	Korsmeyer–Peppas
F3 0.6N (4.5)	2.8891	0.9914	0.9829	−0.0217	0.9969	0.9939	15.5919	0.9907	0.9815	6.7983	0.9990	0.9980	0.76	Korsmeyer–Peppas
F3 0.8N (4.5)	2.7972	0.9865	0.9731	−0.0205	0.9994	0.9989	15.2167	0.9937	0.9874	7.0958	0.9991	0.9982	0.74	First order
F3 1.0N (4.5)	2.5881	0.9904	0.9809	−0.0205	0.9994	0.9989	13.9935	0.9915	0.9832	6.7280	0.9998	0.9997	0.72	Korsmeyer–Peppas

Insertions in parentheses indicate the dissolution media used; 1.5 and 4.5 are indicative of buffers pH 1.5 and 4.5
HCl hydrochloric acid, *F1 0.2N* formulation F1 synthesized in 0.2 N acetic acid, *F3 0.4N* formulation F3 synthesized in 0.4 N acetic acid, etc.

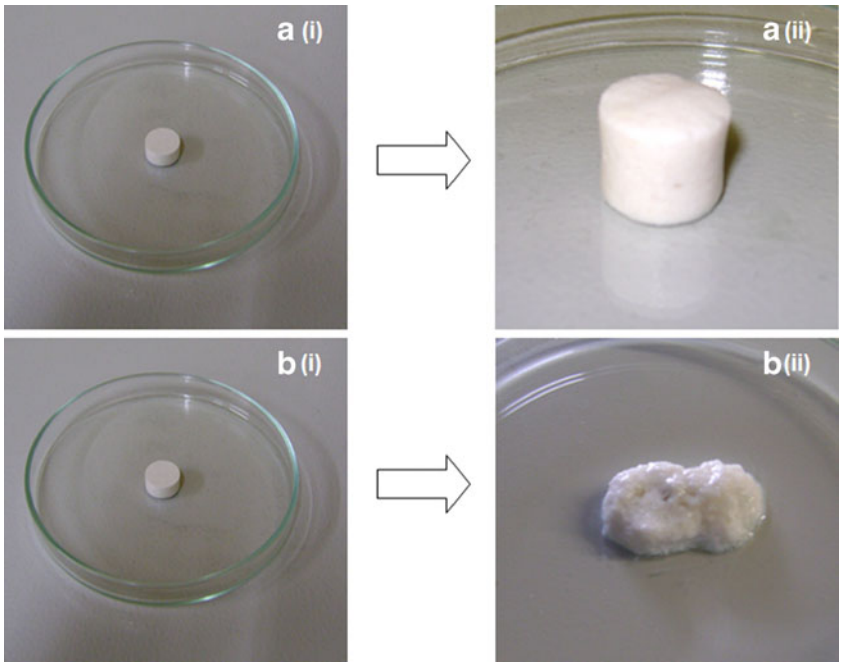

Fig. 7. Digital images of F3 matrices in different pH media: **a** *i–ii* matrix before and after *in vitro* drug release study in pH 1.5, respectively, and **b** *i–ii* matrix before and after *in vitro* drug release study in pH 4.5, respectively

Where Q_t is the quantity of drug release in time t, Q_0 is the initial quantity of drug in dissolution medium which is usually zero and K_1 is the first-order constant. The first-order constant and regression square were obtained by plotting the log of cumulative quantity remaining ($\log(Q_0 - Q_t)$ *versus* time.

Drug release profiles obtained in dissolution media of HCl and buffer pH 1.5 best-fitted first-order release kinetics. However, the release profiles of formulations F3 in buffer pH 4.5 best-fitted zero-order release kinetics as shown in Table VI. Furthermore, the drug release profiles were fitted to Higuchi and Korsmeyer–Peppas equations, and the overall best-fit model was obtained for each formulation. Typically, the Higuchi equation is based on Fick's law of diffusion and is shown in Eq. 4.

$$Q = K_H t^{1/2} \tag{4}$$

Where Q is quantity of drug released per time t, and K_H is Higuchi dissolution constant which is obtained by plotting cumulative percentage or fractional drug release *versus* square root of time (26).

The Korsmeyer–Peppas Equation as expressed in Eq. 5 was employed to evaluate the mechanism of drug release. The equation was used to explicate the drug release pattern from the IPEC-based matrix when the mechanism of release is not well known or more than one release mechanism is entailed (27).

$$Q_t/Q_\infty = K_t^n \tag{5}$$

Where Q_t/Q_∞ is the fractional drug release per time t, K is the constant indicating the structural and geometric characteristics of the matrix, and n is the release exponent. K and n were obtained in accordance with Eq. 6 by plotting the log of percentage drug released (<60%) against the log of time (26).

$$\log [Q_t/Q_\infty] = \log\ K + n\ \log\ t \tag{6}$$

For a cylindrical matrix, the release mechanism is Fickian diffusion if n=0.45, non-Fickian release or anomalous transport if $0.45<n<0.89$, case II transport or zero-order release if n=0.89, and super case II transport if >0.89 (26,27). The values of the release exponent obtained for the IPEC-based matrices are shown in Table VI. Majority of the IPEC-based matrices fitted with the Korsmeyer–Peppas model and all values of the release exponent n were indicative of anomalous transport since the constants were within $0.45<n<0.89$. The exponent values n are indicative that the drug release pattern involved a combination of mechanisms as observed experimentally and explicated earlier in this manuscript.

Prediction of the Mucoadhesive Potential of the IPEC-Based Gastroretentive Matrix

The global energy relationships for the various IPEC complexes derived after AMBER 3 are shown in Eqs. 7–9.

$$E_{\mathrm{PLLN}} = -8.370V_b = 2.275V_b + 19.829V_\theta + 32.087V_\varphi + 11.438V_{\mathrm{ij}} - 4.238V_{\mathrm{hb}} - 69.762V_{\mathrm{el}} \tag{7}$$

$$E_{\mathrm{PDTR}} = -166.812V_b = 5.474V_b + 70.351V_\theta + 55.173V_\varphi - 29.066V_{\mathrm{ij}} - 7.096V_{\mathrm{hb}} - 261.649V_{\mathrm{el}} \tag{8}$$

$$E_{\mathrm{PLLN-PDTR}} = -232.836V_b = 7.997V_b + 94.503V_\theta + 92.414V_\varphi - 32.182V_{\mathrm{ij}} - 10.993V_{\mathrm{hb}} - 384.576V_{\mathrm{el}} \tag{9}$$

$$\Delta E = -57.654\ \mathrm{kcal/mol}$$

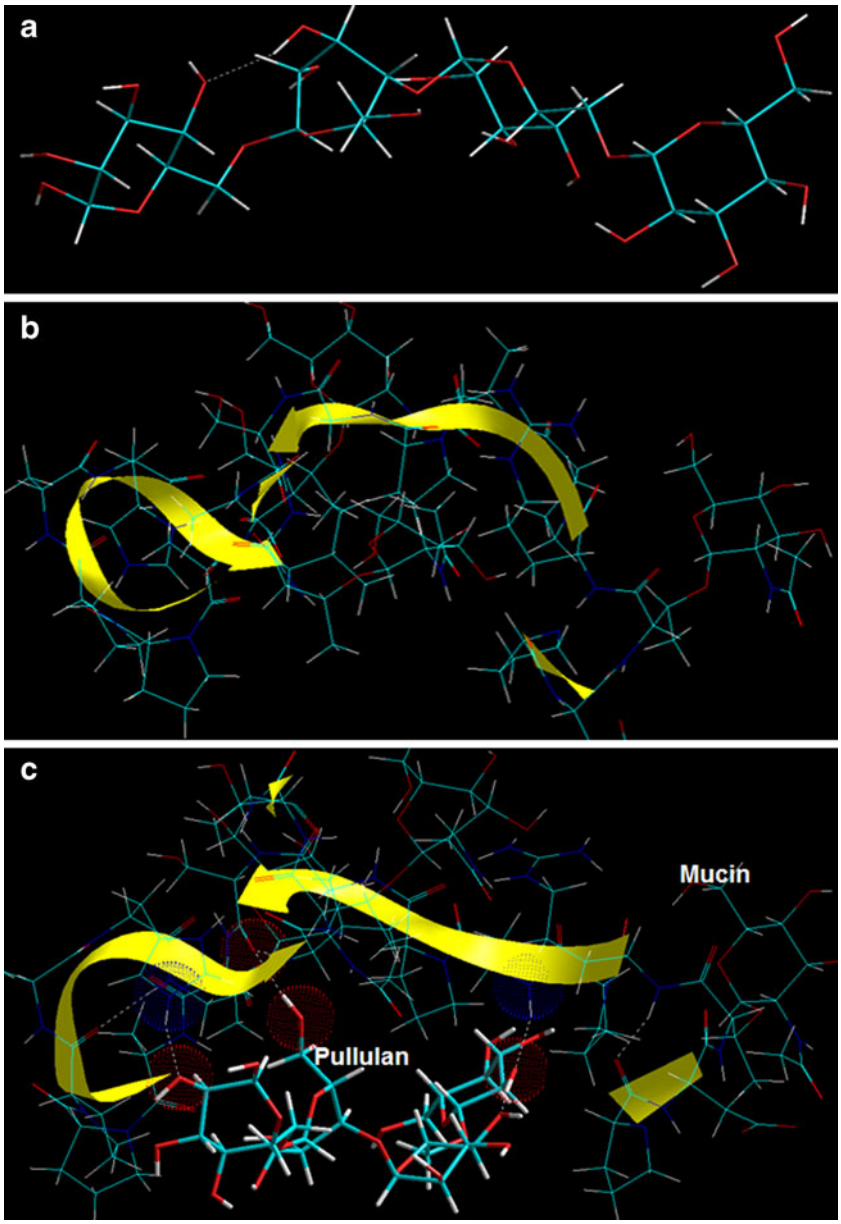

Fig. 8. Visualization of energy minimized geometrical preference of **a** pullulan, **b** glycosylated mucin, and **c** pullulan in complexation with mucin after molecular mechanics simulations. Color codes: C (*cyan*), O (*red*), N (*blue*), and H (*white*)

Table VII. Computed Molecular Attributes of Complexes Involving PLLN, MUC, and PLLN-MUC

Molecular attributes	Molecular complex(s)		
	PLLN	MUC	PLLN-MUC ($\sum$)
Minimized energy (kcalmol^{-1})	−8.370	−166.812	−232.836 (−175.182)
Polarizability ($Å^3$)	55.10	234.89	286.37 (289.99)
Refractivity ($Å^3$)	133.16	581.10	709.25 (714.26)
Volume ($Å^3$)	1,537.50	5,164.82	6,200.90 (6,702.32)
Mass (amu)	666.58	2,479.62	3,146.20 (3,146.20)
Density	0.433	0.480	0.507 (0.469)
Surface area (grid; $Å^2$)	848.62	2,140.88	2,384.89 (2,989.5)
Surface-to-volume ratio	0.552	0.414	0.385 (0.446)

PLLN pullulan, *MUC* mucopeptide analogue, $\sum$ summation of individual molecular attributes,

The bioadhesive or mucoadhesive potential of the IPEC-based matrix was elucidated as a measure of specific chemical interactions between PLLN and the glycosylated MUC after geometrical optimization using energy minimizations. PLLN is known to be a mucoadhesive polymer (28,29) and may impart bioadhesion to the matrix. The energy minimizations were found to be a collective phenomenon including nonbonding interactions in the form of van der Waals forces, H bonding and electrostatic interactions (Eqs. 7–9). This contributed to a stress transduction requiring a large fraction of the surface to establish connectivity between chemically transformed regions. The binding energy of the PLLN with MUC was quite high with ΔE ~58kcal/mol confirming the significant interactions among the molecular entities (Fig. 8). A deeper inspection shows that the specificity of this complex arises due to –CO…NH_2– and –CO…OH– interactions of the PLLN and mucopeptide residue, respectively (Fig. 8c).

In addition, the molecular attributes in terms of surface-to-volume ratio (SVR) and final density corroborated with the experimental mucoadhesive findings with PLLN-MUC having a lower SVR than that of either of the molecules individually (Table VII). The lower the SVR, the more stable was the structure. Furthermore, in the present case, initial models were built using a density derived from the average of that of the pure components. For the polymer-mucopeptide system, a substantial increase in density was observed as compared with the average of the individual molecules involved, with density values from 0.433 through 0.480 to 0.507 amu/Å^3 for PLLN, MUC, and PLLN-MUC, respectively. This density increase was in agreement with the occurrence of specific interchain interactions leading to the mucoadhesivity of the IPEC-based matrix (30). Furthermore, a significant contribution was also provided by the strong H bonding in PLLN-MUC with a bond lengths of <2 Å. These interactions involving the nonbonded attractive forces induced dipoles in the IPEC complex where the binding energy changes was proportional to the polarizability of the substituents, which are in turn proportional to molar refractivity values where the structure with the lower index of refraction was more stable (Table VII). Thus it was concluded that the energy stabilization, low SVR, high density, lower polarizability and lower refractivity lead to highly efficient interactions between the IPEC and the mucosa. These results are in line with the previously reported observations, where the mucoadhesivity of a polymer was defined in terms of the propensity of the molecules set up polar and H-bonding interactions (31). The experimental mucoadhesion studies can be correlated to these *in silico* findings as we propose that PLLN may swell readily in contact with hydrated mucous membranes and become progressively rubbery due to uncoiling of polymer chains which may further result in increased mobility of the polymer chains producing a large adhesive surface for maximum contact with the mucosa and flexibility for interpenetration with the mucosa (32). In addition, a few of the characteristics that are responsible for increased hydrogel mucoadhesive properties include (1) high quantity of H-bonding chemical groups (hydroxyls and carboxyls), (2) anionic surface charges, (3) high polymer molecular mass, (4) high polymer chain flexibility, and (5) surface tensions that will induce spreading into the mucus layer (33).

CONCLUSIONS

A triple mechanism-based gastroretentive drug delivery system has been developed with the potential for improving the absorption and bioavailability of levodopa at a constant rate over prolonged period of time. It is envisaged that the constant delivery of levodopa as observed *in vitro* may ensure constant plasma concentrations and sustained release thereby providing an optimal therapeutic effect. The IPEC synthesized as the gastroretentive platform with a stoichiometrical ratio of 0.5:1 (EUD/NaCMC) proved to have the most superior physicochemical and physicomechanical properties to suit pH-responsive zero-order gastroretentive drug delivery. These properties were distinctly and preferably different from the native polymers. The IPEC produced a stimuli-responsive hydrogel which retained its three-dimensional network in the gastric pH and exhibited excessive swelling to enhance gastroretention. The IPEC also facilitated the production of a denser matrix and exhibited release of levodopa at a constant rate from the matrix. Furthermore, it is anticipated that the three mechanisms of gastroretention viz. swelling, bioadhesion, and high density employed in the IPEC-based matrix designed in this study will be able to prolong the gastric residence time for narrow absorption window drugs such as levodopa.

REFERENCES

1. Birkmayer W, Hornykiewicz O. Der l-3,4-dioxyphenylalanin (=DOPA)-Effekt bei Parkinson-Akinese. Wien Klin Wochenschr. 1961;73:787–8.
2. Muzzi C, Bertocci E, Terzuoli L, Porcelli B, Ciari I, Pagani R, *et al.* Simultaneous determination of serum concentrations of levodopa, dopamine, 3-*O*-methyldopa and α-methyldopa by HPLC. Biomed Pharmacother. 2008;62:253–8.
3. Jankovic J. Levodopa strengths and weaknesses. Neurology. 2002;58:S19–32.
4. Sagar KA, Smyth MR. Bioavailability studies of oral dosage forms containing levodopa and carbidopa using column-switching chromatography followed by electrochemical detection. Analyst. 2000;125:439–45.
5. Koller WC, Hutton JT, Tolosa E, Capilldeo R. Immediate-release and controlled-release carbidopa/levodopa in PD: a 5-year randomized multicenter study. Neurology. 1999;53:1012.
6. Ngwuluka N, Pillay V, Du Toit LC, Ndesendo V, Choonara Y, Modi G, *et al.* Levodopa delivery systems: advancements in delivery of the gold standard. Expert Opin Drug Deliv. 2010;7:203–24.
7. Arza R, Gonugunta C, Veerareddy P. Formulation and evaluation of swellable and floating gastroretentive ciprofloxacin hydrochloride tablets. AAPS PharmSciTech. 2009;10:220–6.
8. Klausner EA, Eyal S, Lavy E, Friedman M, Hoffman A. Novel levodopa gastroretentive dosage form: *in-vivo* evaluation in dogs. J Control Release. 2003;88:117–26.
9. Goole J, Vanderbist F, Amighi K. Development and evaluation of new multiple-unit levodopa sustained-release floating dosage forms. Int J Pharm. 2007;334:35–41.
10. Goole J, Deleuze P, Vanderbist F, Amighi K. New levodopa sustained-release floating minitablets coated with insoluble acrylic polymer. Eur J Pharm Biopharm. 2008;68:310–8.
11. Kumar P, Pillay V, Choonara YE, Modi G, Naidoo D, du Toit LC. In Silico theoretical molecular modeling for Alzheimer's disease: the nicotine-curcumin paradigm in neuroprotection and neurotherapy. Int J Mol Sci. 2011;12:694–724.
12. Camacho MM, Martínez-Navarrete N, Chiralt A. Rheological characterization of experimental dairy creams formulated with locust bean gum (LBG) and λ-carrageenan combinations. Int Dairy J. 2005;15:243–8.

13. Sittikijyothin W, Torres D, Gonçalves MP. Modelling the rheological behaviour of galactomannan aqueous solutions. Carbohydr Polym. 2005;59:339–50.
14. Bardonnet PL, Faivre V, Pugh WJ, Piffaretti JC, Falson F. Gastroretentive dosage forms: overview and special case of *Helicobacter pylori*. J Control Release. 2006;111:1–18.
15. Chawla G, Gupta P, Koradia V, Bansal AK. Gastroretention: a means to address regional variability in intestinal drug absorption. Pharm Technol. 2003;27:50–68.
16. Davis SS, Hardy JG, Fara JW. Transit of pharmaceutical dosage forms through the small intestine. Gut. 1986;27:886–92.
17. Nur A, Zhang J. Captopril floating and/or bioadhesive tablets: design and release kinetics. Drug Dev Ind Pharm. 2000;26:965.
18. Lee JW, Park JH, Robinson JR. Bioadhesive-based dosage forms: the next generation. J Pharm Sci. 2000;89:850–66.
19. Thirawong N, Kennedy RA, Sriamornsak P. Viscometric study of pectin–mucin interaction and its mucoadhesive bond strength. Carbohydr Polym. 2008;71:170–9.
20. Vasir JK, Tambwekar K, Garg S. Bioadhesive microspheres as a controlled drug delivery system. Int J Pharm. 2003;255:13–32.
21. O'Brien S, Wang Y, Vervaet C, Remon JP. Starch phosphates prepared by reactive extrusion as a sustained release agent. Carbohydr Polym. 2009;76:557–66.
22. Kim SW, Bae YH, Okano T. Hydrogels: swelling, drug loading, and release. Pharm Res. 1992;9:283–90.
23. Wise DL, Trantolo DJ, Altobelli DE, Yaszemski MJ, Gresser JD, Schwartz ER. Encyclopedic handbook of biomaterials and bioengineering. 1st ed. Sheffield: Marcel Dekker; 1995. p. 3760.
24. Siepmann J, Göpferich A. Mathematical modeling of bioerodible, polymeric drug delivery systems. Adv Drug Deliv Rev. 2001;48:229–47.
25. Faisant N, Siepmann J, Benoit JP. PLGA-based microparticles: elucidation of mechanisms and a new, simple mathematical model quantifying drug release. Eur J Pharm Sci. 2002;15:355–66.
26. Merchant H, Shoaib H, Tazeen J, Yousuf R. Once-daily tablet formulation and *in vitro* release evaluation of cefpodoxime using hydroxypropyl methylcellulose: a technical note. AAPS PharmSciTech. 2006;7:E178–83.
27. Sriamornsak P, Thirawong N, Weerapol Y, Nunthanid J, Sungthongjeen S. Swelling and erosion of pectin matrix tablets and their impact on drug release behavior. Eur J Pharm Biopharm. 2007;67:211–9.
28. Greaves JL, Wilson CG. Treatment of diseases of the eye with mucoadhesive delivery systems. Adv Drug Deliv Rev. 1993;11:349–83.
29. Jelinek M, Cristescu R, Axente E, Kocourek T, Dybal J, Remsa J, *et al*. Matrix assisted pulsed laser evaporation of cinnamate-pullulan and tosylate-pullulan polysaccharide derivative thin films for pharmaceutical applications. Appl Surf Sci. 2007;253:7755–60.
30. Abou-Rachid H, Lussier L, Ringuette S, Lafleur-Lambert X, Jaidann M, Brisson J. On the correlation between miscibility and solubility properties of energetic plasticizers/polymer blends: modeling and simulation studies. Propell Explos Pyrot. 2008;33:301–10.
31. Murphy C, Pillay V, Choonara Y, du Toit L, Ndesendo V, Chirwa N, *et al*. Optimization of a dual mechanism gastrofloatable and gastroadhesive delivery system for narrow absorption window drugs. AAPS PharmSciTech. 2012;13(1):1–15.
32. Kumar P, Bhatia M. Functionalization of chitosan/methylcellulose interpenetrating polymer network microspheres for gastroretentive application using central composite design. PDA J Pharm Sci Technol. 2010;64:497–506.
33. Kumar P, Singh I. Formulation and characterization of tramadol-loaded IPN microgels of alginate and gelatin: optimization using response surface methodology. Acta Pharm. 2010;60:295–310.